

NASA/TM—2010–216449



# **Welding As Science: Applying Basic Engineering Principles to the Discipline**

*A.C. Nunes, Jr.*

*Marshall Space Flight Center, Marshall Space Flight Center, Alabama*

---

*October 2010*

## The NASA STI Program...in Profile

Since its founding, NASA has been dedicated to the advancement of aeronautics and space science. The NASA Scientific and Technical Information (STI) Program Office plays a key part in helping NASA maintain this important role.

The NASA STI Program Office is operated by Langley Research Center, the lead center for NASA's scientific and technical information. The NASA STI Program Office provides access to the NASA STI Database, the largest collection of aeronautical and space science STI in the world. The Program Office is also NASA's institutional mechanism for disseminating the results of its research and development activities. These results are published by NASA in the NASA STI Report Series, which includes the following report types:

- **TECHNICAL PUBLICATION.** Reports of completed research or a major significant phase of research that present the results of NASA programs and include extensive data or theoretical analysis. Includes compilations of significant scientific and technical data and information deemed to be of continuing reference value. NASA's counterpart of peer-reviewed formal professional papers but has less stringent limitations on manuscript length and extent of graphic presentations.
- **TECHNICAL MEMORANDUM.** Scientific and technical findings that are preliminary or of specialized interest, e.g., quick release reports, working papers, and bibliographies that contain minimal annotation. Does not contain extensive analysis.
- **CONTRACTOR REPORT.** Scientific and technical findings by NASA-sponsored contractors and grantees.
- **CONFERENCE PUBLICATION.** Collected papers from scientific and technical conferences, symposia, seminars, or other meetings sponsored or cosponsored by NASA.
- **SPECIAL PUBLICATION.** Scientific, technical, or historical information from NASA programs, projects, and mission, often concerned with subjects having substantial public interest.
- **TECHNICAL TRANSLATION.** English-language translations of foreign scientific and technical material pertinent to NASA's mission.

Specialized services that complement the STI Program Office's diverse offerings include creating custom thesauri, building customized databases, organizing and publishing research results...even providing videos.

For more information about the NASA STI Program Office, see the following:

- Access the NASA STI program home page at <<http://www.sti.nasa.gov>>
- E-mail your question via the Internet to <[help@sti.nasa.gov](mailto:help@sti.nasa.gov)>
- Fax your question to the NASA STI Help Desk at 443-757-5803
- Phone the NASA STI Help Desk at 443-757-5802
- Write to:  
NASA STI Help Desk  
NASA Center for AeroSpace Information  
7115 Standard Drive  
Hanover, MD 21076-1320

NASA/TM—2010–216449



# **Welding As Science: Applying Basic Engineering Principles to the Discipline**

*A.C. Nunes, Jr.*

*Marshall Space Flight Center, Marshall Space Flight Center, Alabama*

National Aeronautics and  
Space Administration

Marshall Space Flight Center • MSFC, Alabama 35812

---

**October 2010**

## Acknowledgments

This Technical Memorandum (TM) discusses technical issues that the author encountered as a member of the welding group at Marshall Space Flight Center. His usual role was that of analyst, interpreting phenomena in terms of physical models and attempting to 'put things together.' Over the years, skilled technicians solved most of the technical problems that emerged, without need of the author's help. In cases where the author was involved, the Processes Development team of engineers and technicians (and sometimes the Materials Diagnostic team of the Metals Engineering Branch) planned and carried out empirical studies. A Summer Faculty program provided a pool of colleagues who carried out various research projects and contributed their considerable expertise. Occasional contractors also contributed, such as Susan Hessler of Jacobs Engineering, Science, and Technical Services Group/Snyder Technical Services, who performed an initial edit of this TM. Lately, the Intergovernmental Personnel Act has supplied the benefit of colleague Dr. Judy Schneider of Mississippi State University. In short, the author is indebted to a great many people and grateful to them all.

Available from:

NASA Center for AeroSpace Information  
7115 Standard Drive  
Hanover, MD 21076-1320  
443-757-5802

This report is also available in electronic form at  
<<https://www2.sti.nasa.gov>>

## TABLE OF CONTENTS

1. INTRODUCTION .....	1
1.1 Philosophical Preface.....	1
1.2 Conceptual Models.....	1
1.3 Mathematical Models.....	1
1.4 Statistical Models .....	2
1.5 Symbolic Logic.....	2
2. PENETRATION AND LACK OF PENETRATION .....	3
2.1 Variability of Penetration .....	3
2.2 Monopole Heat Sources .....	3
2.3 Dipole Heat Sources and Phase Change .....	4
2.4 Quadrupole Heat Sources and Weld Pool Currents .....	4
2.5 Marangoni Circulations and Penetration Variability .....	5
2.6 Penetration by Plasmas and High-Power Density Beams .....	5
3. A MECHANISM FOR MICROFISSURES.....	7
3.1 Transient Thermal Stresses .....	7
3.2 Liquid Film Embrittlement .....	9
4. DEFECTS OR ENIGMAS?.....	11
4.1 What is an Enigma? .....	11
4.2 Segregation Enigmas .....	11
4.3 Diffraction Enigmas .....	12
5. THE PLASMA TORCH THAT WOULD NOT SHIELD .....	15
5.1 Porosity in Aluminum Alloy Welds .....	15
5.2 Variable Polarity Plasma Arc Welding .....	15
5.3 The Strength of Variable Polarity Plasma Arc Welds .....	16
5.4 Shield Gas Turbulence .....	16
6. SPARKING AND SPATTER IN SPACE .....	18
6.1 The Soviet Universal Hand Tool .....	18
6.2 Arcs and Paschen Curves .....	19
6.3 Weld Spatter .....	20

## TABLE OF CONTENTS (Continued)

7. WELDING WITHOUT MELTING .....	22
7.1 The British Friction Stir Welding Process .....	22
7.2 How Does Friction Stir Welding Work? .....	23
7.3 A Kinematic Model of Friction Stir Welding Metal Flow .....	24
7.4 Particle Interactions .....	26
7.5 Torque and Drag Forces .....	26
7.6 Weld Defects .....	27
8. CONCLUSION .....	29
REFERENCES.....	30

## LIST OF FIGURES

1.	A broadening temperature profile can cause central regions of a weld to contract while peripheral regions expand. Stresses at the juncture of these regions can cause microfissures in electron beam welds .....	8
2.	Simplified model of cracking at liquated grain boundary. It occurs within a temperature range where tension below that causing plastic metal flow is sufficient to overcome surface tension forces holding the liquid layer in place. An embrittled liquid layer does not actually rupture until a certain amount of strain is imposed upon it .....	9
3.	Filaments of segregation can be produced by a combination of solidification effects and pressure-induced flows of liquids in partially solidified alloys. These filaments are hard to observe using metallographic techniques, but can be seen as segregation ‘enigmas’ using radiography .....	12
4.	Diffraction effects from large grains can shift a noticeable portion of the power of a radiographic beam by a small angle. At one edge of the diffracted image of the grain, the shifted power adds to the background radiation, producing a dark image. At the other edge, the diffracted image subtracts, producing a light line. These boundaries are diffraction ‘enigmas,’ sharply enough defined to be visible when the edge of a large grain lines up parallel to the beam direction ....	14
5.	The external shape of a plasma jet nozzle makes a difference in torch performance. A spherical shape allows the wake separation point to move close enough to the shield gas surface at high flow rates for the wake turbulence to entrain atmospheric contamination (and lose shielding). A conical shape confines the turbulent wake deep within the shield gas flow, avoiding atmospheric entrainment even at high shield gas flows .....	17
6.	The Paschen curve $V = V(Pd)$ bounds the values of voltage ( $V$ ), pressure ( $P$ ), and gap width ( $d$ ) for which arcing occurs in a specific gas. To the right, electron collisions occur so frequently with the gas that they do not build up enough kinetic energy to knock out other electrons. To the left, there are too few gas atoms in the gap for significant multiplication of electrons .....	20
7.	In friction stir welding, a rotating pin stirs the sides of a weld seam together. A shoulder prevents the upwelling of metal around the pin, which would result in plowing, not welding. In conventional FSW, a large plunge force maintains proper shoulder contact; it is balanced by a heavy fixed anvil underneath the work-piece. In self-reacting FSW, a pinch force maintains proper shoulder contact, making a heavy supporting anvil unnecessary .....	23

## LIST OF FIGURES (Continued)

8. Plan view of trace of seam around pin during FSW in simplified two-dimensional flow model. An eccentricity  $\delta$  of the shear surface accommodates the backflow of metal around the pin. Metal inflow volume en route at weld speed  $V$  for a shear surface of unit height and radius  $R$  is  $2RV$ . Backflow at the outer edge of a plug of metal rotating with the tool at angular velocity is  $\delta R\Omega$  ..... 24

## LIST OF ACRONYMS AND SYMBOLS

ASEE	American Society for Engineering Education
Cu	copper
ESTS	engineering, science, and technical services
FSW	friction stir welding
GTA	gas tungsten arc (welding)
ISWE	International Space Welding Experiment
Li	lithium
Mn	manganese
MSU	Mississippi State University
NDE	nondestructive evaluation
Si	silicon
SMAW	shielded metal arc welding
TM	Technical Memorandum
UHT	Universal Hand Tool
VPPA	variable polarity plasma arc (welding)

## NOMENCLATURE

$d$	distance; gap width
$F_d$	drag force
$k$	thermal conductivity
$L$	length
$M$	torque
$P$	power; pressure
$R$	radius, fixed
$r$	radius, varying
$T$	temperature
$T_m$	melting temperature
$T_o$	ambient temperature
$V$	voltage; weld speed; velocity
$v$	radial velocity component in friction stir welding
$w$	thickness of plate
$x$	coordinate along direction of motion
$y$	lateral coordinate perpendicular to $x$ -coordinate in plane of weld
$Z$	axial penetration distance
$z$	axial coordinate perpendicular to $x$ - $y$ plane of weld
$\Delta\delta_C$	thickness increase causing rupture in intergranular liquid film
$\Delta t$	time increment
$\delta$	thickness of intergranular liquid film; additional radial thickness of friction stir welding rotating plug on retreating side of tool which accommodates weld metal backflow
$\varepsilon_C$	critical strain causing rupture in intergranular liquid film
$\theta$	angle from direction of motion positive
$\mu$	surface tension
$\mu_d$	dipole heat source
$\mu_q$	quadrupole heat source
$\sigma_F$	normal flow stress of weld metal
$\tau$	shear flow stress of weld metal
$\Omega$	angular velocity of friction stir welding tool
$\omega$	angular velocity of friction stir welding rotating plug

## TECHNICAL MEMORANDUM

### WELDING AS SCIENCE: APPLYING BASIC ENGINEERING PRINCIPLES TO THE DISCIPLINE

#### 1. INTRODUCTION

For those who know, the discipline of welding is a rich source of technically interesting problems. For those who do not know, this Technical Memorandum (TM) describes sample problems illustrating ways in which basic engineering science has been applied to the discipline of welding. Perhaps inferences may be drawn regarding optimal approaches to particular welding problems, as well as for the optimal education of welding engineers. Perhaps also some readers may be attracted to the science(s) of welding and may make worthwhile contributions to the discipline.

##### 1.1 Philosophical Preface

Arguably, the normal mode of welding evolution is by cut-and-try methods at the level of the welding technician. ‘All men by nature desire to know,’ but the world is not likely to provide funding unless the potential exists for a commercial payoff. However, technicians sometimes encounter problems that they are unable to solve. Sometimes, too, a broader perspective is wanted to help give direction to the developmental process; then, scientific methodology may be called upon for assistance. ‘Science’ entails a clear idea of the way in which the process works with implications as to how to achieve the desired results; i.e., understanding the situation. An appropriate approach is required to achieve understanding, and it is not always obvious either.

##### 1.2 Conceptual Models

Conceptual models—essentially visualizations—may be considered intrinsic to an understanding of any process. Conceptual modeling is an old faculty that is shared in greater or lesser degree with other sentient animals, primed through education in a variety of technical specializations, and facilitated through general education in language, which includes visual, auditory, and tactile perceptions. But understanding cannot be forced. Problems are ingested and then what will emerge emerges. Given an adequate level of mental composure and a healthy physical constitution, advance preparation is the crux of the ability to solve problems and is critical. Technical breadth is important; overspecialization may prematurely fix on an unfruitful approach.

##### 1.3 Mathematical Models

Mathematical models may be useful per se or merely as a means to select among alternate conceptual models. Models may be classified by how much mathematical apparatus or abstraction

exists between the model implementation and a simple visualization. The geometrical mechanics of Newton's *Principia* (1687)<sup>1</sup> is a more visually direct approach to mechanics than Lagrange's *Mécanique analytique* (1788)<sup>2</sup> in which the potential (a new mathematical apparatus invented by Lagrange) plays a major role in mechanical modeling. Since then, potentials have become so popular that they have become fundamental constituents of our models of the world (as energy, entropy, temperature, etc.) and their construct nature tends to be forgotten.

The popular finite element models incorporate so much mathematical apparatus between starting assumptions and predicted system behavior that one is likely to have to remodel the finite element model in terms of a less elaborate model in order to understand it. Finite element models may present extremely detailed information, but modeling errors may produce deceptive artifacts. In the author's opinion, finite element analyses are best used for detailed representations of well understood systems while, for exploratory studies, it is best to begin with an assemblage of the simplest possible modeling elements that might represent the target system.

#### **1.4 Statistical Models**

Statistical models are perhaps best used as clues for constructing conceptual models. Statistical models per se do not provide understanding as do conceptual models. Statistical models depend upon often unconscious—and never guaranteed—global assumptions about the systems being analyzed; conclusions are in terms of odds for particular outcomes dependent upon the global assumptions. Statistics can deceive if one is not very clear on what has been assumed and what the statistical conclusion really means.

In the course of a study of microfissuring in electron beam welds, the author encountered a statistical study that asserted suppression of microfissuring by manganese (Mn) in excess of 0.2% and silicon (Si) in excess of 0.25%.<sup>3</sup> A second study asserted promotion of microfissuring by Mn and Si in excess of 0.15%.<sup>4</sup> These apparently contradictory yet statistically based conclusions impressed the author with a skeptical attitude regarding statistics.

#### **1.5 Symbolic Logic**

Symbolic logic can be useful on occasion. The author can recall an instance where a truth table helped sort out the implications of a complex set of observations. A predilection for philosophy and its tools for thinking is an asset for weld analysis. The business of philosophers is to make things clear.

It may be added that an overly reverential attitude toward prior ideas may be an obstacle to a correct understanding of a phenomenon of interest. The analyst needs the confidence engendered by fluency in his/her disciplines, fluency such as a teacher acquires. A background in the historical development of science and technology in general (and the subject technology in particular) also imparts confidence, as well as the occasional good idea. However, confidence is not incompatible with humility, and falling in love with one's theoretical constructions can lead to theoretical catastrophe.

## 2. PENETRATION AND LACK OF PENETRATION

The usual image evoked by the word ‘welding’ is probably a little pool of molten metal beneath a dazzling electric arc, being coaxed along a metal seam by a helmeted welder peering out through a very dark glass. The molten metal solidifies behind the weld pool to the depth penetrated by the pool, leaving solid metal in place of an open seam. The seam—or part of it—is now welded.

If the weld does not penetrate the seam completely but instead leaves a bit of seam unwelded, a weld defect known as ‘lack of penetration’ has been made. Lack of penetration can cause a large reduction in the strength of a weld. In critical welded structures, where a failed weld could mean loss of life, it is likely that welds will be checked by a nondestructive evaluation (NDE) procedure, such as x-ray radiography. In radiography, the weld is placed between a source of x rays and a detector (say, x-ray film) and an image of the weld is examined on the detector. Lack of penetration reveals itself as a dark line down the center of the weld. If present, lack of penetration may be ground out and the location rewelded.

### 2.1 Variability of Penetration

But why should all this be necessary? How hard should it be to precisely control penetration? Suppose the arc is produced by a torch that is mounted on a mechanical drive and all the welding parameters are fixed; e.g., electrode standoff distance from the workpiece, electric current, torch speed, shield-gas flow rate, electrode tip shape, etc. for, say, the gas-shielded, nonconsumable tungsten electrode process known as gas tungsten arc (GTA) welding. Even so, weld penetration is so sensitive to slight within-specification variations in alloy composition that a composition-dependent range of depths from 100% to 70% penetration have been observed in mechanized, constant parameter welds in type 304 stainless steel.<sup>5</sup> Heat sinks in the vicinity of the weld can also have a noticeable effect. The author has observed a 69% partial penetration GTA weld in an aluminum alloy reduced to approximately 65% upon being clamped in a fixture and, upon passing close to a hold-down clamp, to approximately 47%.<sup>6</sup> Even a precision mechanized GTA welding apparatus needs to be manned by an experienced welder who can adjust the welding parameters to produce the desired level of penetration.

### 2.2 Monopole Heat Sources

What determines penetration? Why should it be sensitive to weld metal composition? Imagine a heat source of power  $2P$  in an infinite metal continuum of thermal conductivity ( $k$ ); the source raises the temperature ( $T$ ) in its vicinity until the thermal gradient is able to conduct the heat away, after which the local temperature becomes fixed. There being no preferred radial direction in an infinite continuum, the isotherms are spheres surrounding the point heat source. For conduction of heat through the spherical surface at radius ( $r$ ),

$$2P = \left( -k \frac{dT}{dr} \right) 4\pi r^2 . \quad (1)$$

The spherical symmetry ensures that no heat is transferred circumferentially, so the same differential applies to a half continuum with a heat source of power ( $P$ ) on its surface dissipated through area  $2\pi r^2$ . Integration of equation (1) from very large radii, where the temperature is the ambient temperature  $T_o$  to the edge of the molten pool at radius ( $R$ ) and melting temperature ( $T_m$ ) yields a rudimentary estimate of penetration for a slow-moving weld on a large block of metal:

$$R = \frac{P}{2\pi k(T_m - T_o)} . \quad (2)$$

A corresponding solution exists for a faster moving weld, but the weld pool is distorted along the direction of movement and is no longer spherical.<sup>7</sup> An infinite array of heat sources placed  $2w$  apart have planes of symmetry across which there is no transfer of heat, one kind of plane containing a heat source, the other not containing a heat source. The temperature distribution in the space between two dissimilar planes represents that in a plate of thickness ( $w$ ). A three-dimensional array of point sources can be used to represent the temperature distribution in a block of metal bounded on all six sides.

### 2.3 Dipole Heat Sources and Phase Change

But there is more. As the weld moves forward, energy is absorbed in melting metal at the front of the pool and recovered at the rear of the pool as metal solidifies and gives off its latent heat of melting. This phase change effect on temperature may be very simply approximated by adding a dipole heat source ( $\mu_d$ ):

$$(T - T_o)_{\text{dipole}} = -\lim_{\substack{\Delta x \rightarrow 0 \\ \Delta x \Delta P \rightarrow \mu_d}} \frac{\partial}{\partial x} \left( \frac{\Delta P}{2\pi k r} \right) \Delta x = \frac{\mu_d}{2\pi k r^2} \frac{x}{r} . \quad (3)$$

$x$  is the coordinate along the direction of motion while  $r = \sqrt{x^2 + y^2 + z^2}$  is the radial coordinate. The dipole comprises a pair of equal and opposite heat sources of power ( $\Delta P$ ) separated by distance ( $\Delta x$ ). As  $\Delta x$  approaches zero, the strength of the dipole  $\Delta x \Delta P$  approaches  $\mu_d$ .

### 2.4 Quadrupole Heat Sources and Weld Pool Currents

Of greater interest for present purposes is a surface tension effect on the temperature field that can be most simply approximated by a quadrupole field constructed of pairs of equal and opposite dipoles:

$$\begin{aligned} (T - T_o)_{\text{quadrupole}} &= -\lim_{\Delta x \rightarrow 0} \frac{\partial}{\partial x} \left( \frac{\Delta \mu_d}{2\pi k r^2} \frac{x}{r} \right) \Delta x - \lim_{\Delta y \rightarrow 0} \frac{\partial}{\partial y} \left( \frac{\Delta \mu_d}{2\pi k r^2} \frac{y}{r} \right) \Delta y \\ &= \frac{\mu_q}{2\pi k r^3} \left( 1 - 3 \frac{z^2}{r^2} \right) . \end{aligned} \quad (4)$$

Ignoring dipole effects and taking the maximum penetration to occur along the  $z$ -axis by symmetry, penetration  $Z$  comprises the solution to

$$Z^3 - \frac{P}{2\pi k(T_m - T_o)} Z^2 + \frac{\mu_q}{\pi k(T_m - T_o)} = 0 . \quad (5)$$

By differentiation,

$$\left( \frac{dZ}{d\mu_q} \right)_{\mu_q=0} \approx -\frac{2}{PZ} . \quad (6)$$

## 2.5 Marangoni Circulations and Penetration Variability

Increased surface temperature tends to reduce surface tension. The center of the weld pool—where the arc impinges and the heat source is strongest—tends to have a lower surface tension. The resultant surface tension imbalance on the pool surface induces a flow of molten metal from the pool center out to the pool edge. Heat is transferred to the outer edge of the pool by convection (positive  $\mu_q$ ), penetration is reduced, and the pool takes on a wide shallow shape.

Pool surface contamination also tends to reduce surface tension, but contamination is often driven off by heat. If the contamination effect dominates, close to the center of the pool surface, the surface tension is raised. Molten metal is induced to flow toward the pool center and down into the depths of the pool. Heat is transferred to the depths of the pool and the pool takes on a narrow deep shape.

Large variations in penetration due to small variations in alloy composition were explained in 1982 by Heiple and Roper,<sup>8</sup> researchers at Rockwell International, as caused by surface tension gradient-driven currents in the weld pool called Marangoni<sup>9</sup> circulations. Pool circulations can also be driven by other factors, such as electromagnetic induction or gravitational circulation, but the Marangoni circulations generally dominate. Hence, obviously different penetration levels in fusion welding experiments may not be an occasion for drawing conclusions, unless one accounts for the Marangoni circulation effect, and not just in GTA welding.

## 2.6 Penetration by Plasmas and High-Power Density Beams

High-power density electron and laser beams ride up on the forward surface of a vapor cavity. The higher the angle of the forward surface, the greater the area exposed to the beam. The angle increases until the area is sufficient to dissipate the beam power through phase changes (e.g., melting, evaporation) and conduction into the metal; this determines the penetration of the beam. Marangoni forces induce the flow of molten metal to the cooler surfaces behind the beam, where it solidifies and welds the seam together. Faster extraction of molten metal from under the beam removes heat faster and may be expected to reduce penetration and vice versa.

This brief discussion suggests a penetration mechanism that may be sensitive to the power distribution over the cross sections of high-power density beams, which is indeed the case. A slight change in focus of an electron beam may cause a large change in penetration. Laser beams sometimes have irregular cross-sectional power distributions (modal patterns) at higher power levels. These irregularities cause welding problems.

### 3. A MECHANISM FOR MICROFISSURES

Electron beams can concentrate power so densely that when they strike a metal surface, the strike area is not adequate to dissipate the beam energy at temperatures where the metal can remain solid or even liquid. Under a welding electron beam, a metal surface evaporates to form a cavity. The cavity wall makes a steep angle with the beam, and the area under the beam enlarges to a point where the power in the beam can be dissipated at endurable temperatures. A beam moving forward along a metal seam rides up on the forward surface of the vapor cavity, where it melts the metal. The molten metal flows back around the beam, pulled by increased surface tension to the cooler region beside and behind the arc, where it solidifies, leaving a welded seam. Electron beam welds are very narrow and minimize heat damage to the environment. They are made in a vacuum chamber because, outside of very unusual circumstances, the beam will not penetrate air. The vacuum also minimizes risk of contamination from atmospheric constituents. Thus, electron beam welding tends to produce very high-quality welds.

However, electron beam welds have their share of defects also. For example, they can exhibit tiny cracks called microfissures at the edges of the weld, particularly in the region where the nail-head (a broad melted region at the top of the weld) joins the spike (a narrow melted region closely following the vapor cavity of the beam). How might they be eliminated?

Metallurgists, observing that microfissures followed grain boundaries, hypothesized a culprit trace constituent that would promote grain boundary melting. Perhaps the presence of potential scavengers, Mn and Si, would exhibit a beneficial effect on microfissuring? But as noted above,<sup>3,4</sup> this approach was unsuccessful.

#### 3.1 Transient Thermal Stresses

Technicians thought that microfissuring tended to occur at higher weld speeds. Indeed, microfissuring was not observed in the slower arc welds, which suggested that thermal gradients and gradient-related stresses might be a culprit. Further, the crack surfaces were roughly parallel to the weld metal surface, as if opened up by stresses perpendicular to the surface. These data and conjectures suggested a thermal stress model of microfissuring. See figure 1.

It was supposed that the temperature field broadens just behind the beam. The weld begins to cool down at the centerline and heat up away from the centerline. Perpendicular to the plate, the outer metal expands and tends to pull apart the inner metal, which is contracting. (In the plane of the plate, the expanding environment compensates for the contracting inner metal and may even compress it.) If the inner metal is still hot and not completely solidified, grain boundary liquefaction may embrittle the metal, so that it cracks instead of deforming plastically under the deformation forced by differential thermal expansion.

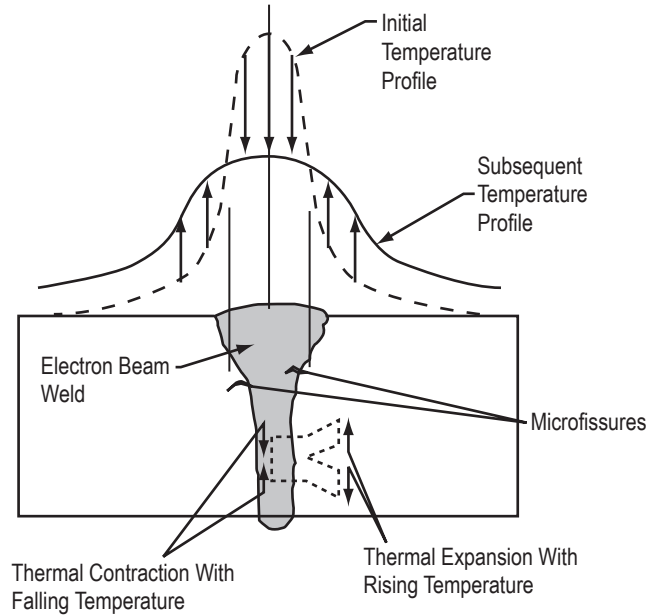


Figure 1. A broadening temperature profile can cause central regions of a weld to contract while peripheral regions expand. Stresses at the juncture of these regions can cause microfissures in electron beam welds.

This model was implemented mathematically. The weld temperature field was approximated by a moving line heat source for the spike and a moving point source for the nailhead.<sup>7</sup> The weld temperature field first subjects a thin column of metal adjacent to the weld to a thermal expansion as it heats up and then to a thermal contraction as it begins to cool. Beyond the column the environment continues to heat up and expand for a bit as the column cools, and, during this time interval, since the column is attached to the environment, the column is forcibly expanded in a succession of plastic strain increments. These plastic strain increments were calculated approximately. The critical strain necessary to cause cracking at a given temperature was determined by observing the strain required to crack the surface of hot tensile specimens at various temperatures. By comparing the computed strains with the critical cracking strains through a ‘damage’ computation it was possible to estimate not only whether a given set of weld parameters would cause microfissuring, but at what weld depth the microfissures would be located.

This crude model worked surprisingly well. Weld parameters such as speed, power, type of process (i.e., electron beam or arc or plasma) were introduced into the model through the temperature profile, and predictions emerged as a computed damage curve through the thickness of the plate. The model showed that microfissures would form in high-speed electron beam welds (but not low-speed arc welds, with reduced transient thermal stresses) at the junction between the spike and the nailhead. Its predictions corresponded well with observed phenomena.

This understanding suggests two methods other than weld parameter adjustment that might be used to eliminate microfissuring: (1) a roller to compress the metal behind the beam and (2) rastering of the beam to reduce transient thermal stresses. However, both would require further

development and, as far as the author is aware, neither has yet been successfully introduced into welding practice.

### 3.2 Liquid Film Embrittlement

Although the original software predicting microfissuring is no longer readable by contemporary computers, equivalent (and doubtless better) software can be constructed based upon the information given here. One thing that the author would do differently today is to try to interpret observations of critical cracking strain in terms of a mechanical model. Suppose that microfissures are a result of the rupture of a thin melted film at a grain boundary. See figure 2. A liquid film of thickness ( $\delta$ ) and surface tension ( $\mu$ ) becomes unstable and begins to ‘unzip’ when subjected to tensile stress:

$$\sigma = \frac{2\mu}{\delta} . \quad (7)$$

This can only happen if the plastic flow stress  $\sigma_F$  of the weld metal is greater than the stress to rupture a grain boundary. Hence, the temperature range in which microfissuring can occur would be determined by

$$\frac{2\mu(T)}{\delta(T)} < \sigma_F(T) . \quad (8)$$

The temperature ( $T$ ) dependencies indicated in inequality (8) are not well known and depend upon the state of microsegregation of the alloy. Interpretations are feasible, but probably not computations from first principles. Within the embrittled range, the liquid in an originally liquid-filled boundary of length ( $L$ ) and width ( $\delta$ ) ruptures when extended to width  $\delta + \Delta\delta_C$  where

$$\Delta\delta_C \approx \sqrt{\frac{L\delta}{\left(1 - \frac{\pi}{4}\right)}} - L . \quad (9)$$

If the grain size and the separation between cracks is  $\sim 2L$ , then an upper bound for the critical strain for forming microfissures  $\epsilon_C$  is

$$\epsilon_C \sim \frac{\Delta\delta_C}{2L} \sim \frac{1}{2} \left[ \sqrt{\frac{1}{\left(1 - \frac{\pi}{4}\right)} \frac{\delta}{L}} - 1 \right] . \quad (10)$$

Appropriate values of  $\epsilon_C$  may be appreciably smaller if the liquid layer does not completely rupture, but solidifies while only partially separated.

Liquation cracking is very common, so detailed studies of the underlying mechanism could be useful. Unfortunately the author is unaware of any such studies.

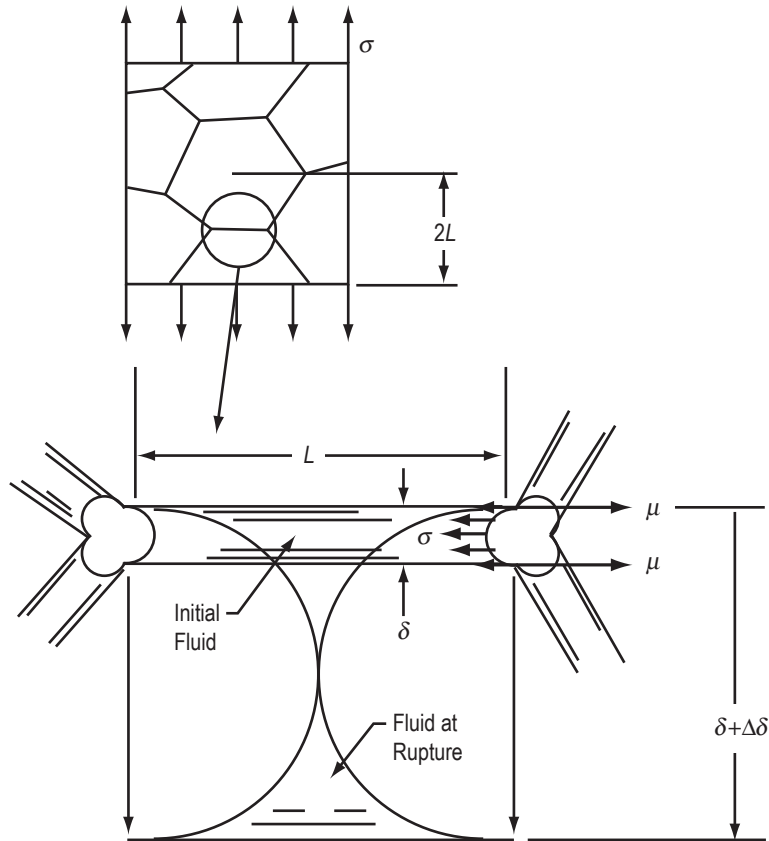


Figure 2. Simplified model of cracking at liquated grain boundary. It occurs within a temperature range where tension below that causing plastic metal flow is sufficient to overcome surface tension forces holding the liquid layer in place. An embrittled liquid layer does not actually rupture until a certain amount of strain is imposed upon it.

## 4. DEFECTS OR ENIGMAS?

Critical welds that cannot be allowed to fail are inspected using NDE methods such as radiography, in which a weld is placed between a source of x rays and x-ray sensitive film. X rays darken film. Hollow spaces in the weld (e.g., porosity or cracks) let through more x rays and produce darker areas on the film. Such radiographs can provide a trained radiographer with a good idea of the soundness of a weld and the kind of defects present, if any.

### 4.1 What is an Enigma?

But what is to be made of a line—usually dark, but sometimes light or mixed light and dark—appearing along the edge of a weld without any apparent cause to be seen when the weld is cut open? Such apparently uncaused radiographic indications are well known to welders as ‘enigmas.’

Space vehicles, in large part, consist of light metal tanks typically fabricated from aluminum alloys. These tanks contain critical welds that are radiographed and, upon the introduction of a new plasma welding process, many ‘straightline enigmas’ began to appear in the welds. A proposal was made to intentionally create a number of these enigmas for testing, in order to determine whether the defective welds would have to be ground out and rewelded—an expensive undertaking at best. But nobody knew how to make the enigmas.

### 4.2 Segregation Enigmas

An embarrassingly long and fruitless series of trial-and-error attempts to find out what might cause ‘straightline enigmas’ ensued. Then a revelation occurred. It came in the form of a radiograph of a slice of the first-pass weld bead not yet covered by a second-pass cover bead. In figure 3, the key features of the radiograph are sketched. Sometimes structural features reduce to the imperceptible on the two dimensions presented by a polished and etched surface, but add up to a visible presence over the third-dimensional length increment of a radiograph.

The crown of the weld pass had a hump in the center and troughs running along the edges of the weld. It is common knowledge among welding engineers that the expanding temperature profile in the wake of a weld causes thermal expansion of the metal outside the weld, which can give a squeeze to the weld even though the weld itself is cooling and shrinking. The radiograph showed a thin light line on the bottom of the troughs, with a complementary dark area below the troughs. Clearly, the thin light line was extruded copper- (Cu-) rich metal, the Cu-rich still-molten constituent of not-quite solidified aluminum-Cu alloy being squeezed by the plate edges. The dark area was the Cu-poor volume, which had supplied the Cu-rich extrusion metal.

When the welders ran a tapered cover pass over the initial pass, they found that the deep end of the pass (higher power) entirely dispersed the segregate and no enigma resulted. The shallow end

of the pass uncovered the bottom of the troughs and produced a genuine defect. But in the middle between the deep and the shallow ends, the thin residual undispersed filament of segregate (usually Cu-poor) produced the observed (usually dark) enigma.

Their nature discovered, production began that day on a batch of enigmas for testing. In the end, ultrasonic testing was required to distinguish them from exposed troughs, but it was no longer considered necessary to grind out and replace the weld metal that produced these enigmas.

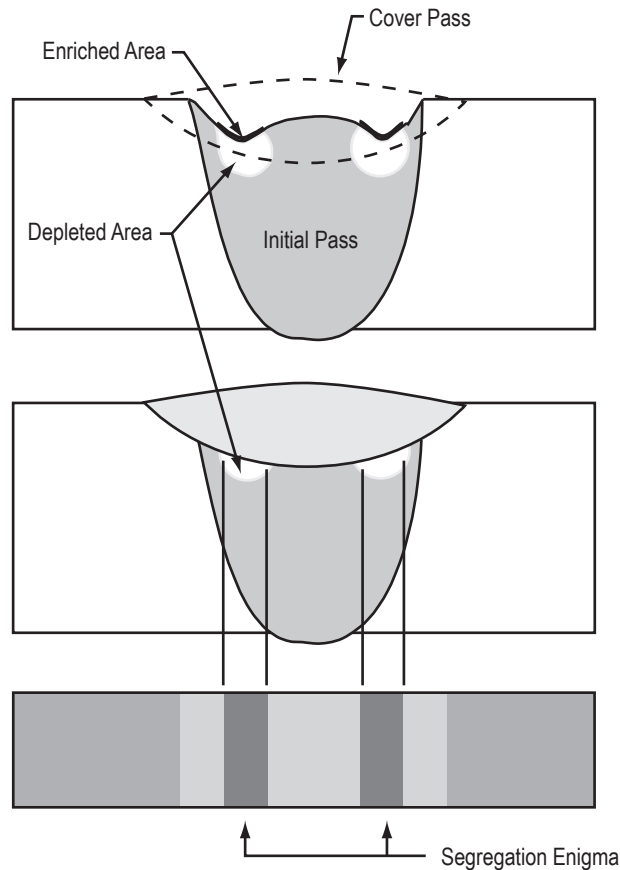


Figure 3. Filaments of segregation can be produced by a combination of solidification effects and pressure-induced flows of liquids in partially solidified alloys. These filaments are hard to observe using metallographic techniques, but can be seen as segregation ‘enigmas’ using radiography.

### 4.3 Diffraction Enigmas

A second kind of enigma is caused not by segregation but by diffraction effects. In one instance, dark lines seen on radiographs of an Inconel 718 duct weld were alleged to be harmless enigmas, not requiring action, by a welding contractor. In response, a study was undertaken to produce and observe enigmas and to determine characteristic features by which diffraction enigmas could be clearly identified.<sup>10</sup>

When a collimated polychromatic x-ray beam impinges upon a single crystal, x rays scattered in certain directions are in phase and add up to produce strong reflected beams. On a detecting surface, the strong reflections produce patterns of spots called Laue patterns, which are typically used to determine the orientation of single crystals. The reflection angles depend upon both crystal structure and orientation. The Laue spots are images of the diffracted beam, the cross section of which is made small for precise spot location.

Slower weld speeds with rounded (not teardrop-shaped) weld puddles tend to promote the formation of large grains running down the center of the weld. The very broad polychromatic radiographic beam encompasses the entire working area including the grains and, in addition to the transmitted beam image, may produce other shifted images of the grain equivalent to Laue spots. If the grain edges are aligned to give sharp boundary images and if the intensity is sufficient, the boundary becomes visible as shown in figure 4. The shifted image reduces the x-ray intensity where it vacates boundary and increases the intensity over the boundary where it is superimposed. Thus, the grain is outlined in dark on one side and in light on the other. These lines are ‘diffraction enigmas.’ Only one side need be sharp enough to be visible. Dark lines—suggesting a possible lack of penetration or a crack—are more ominous than light lines and are the chief concern of an inspector.

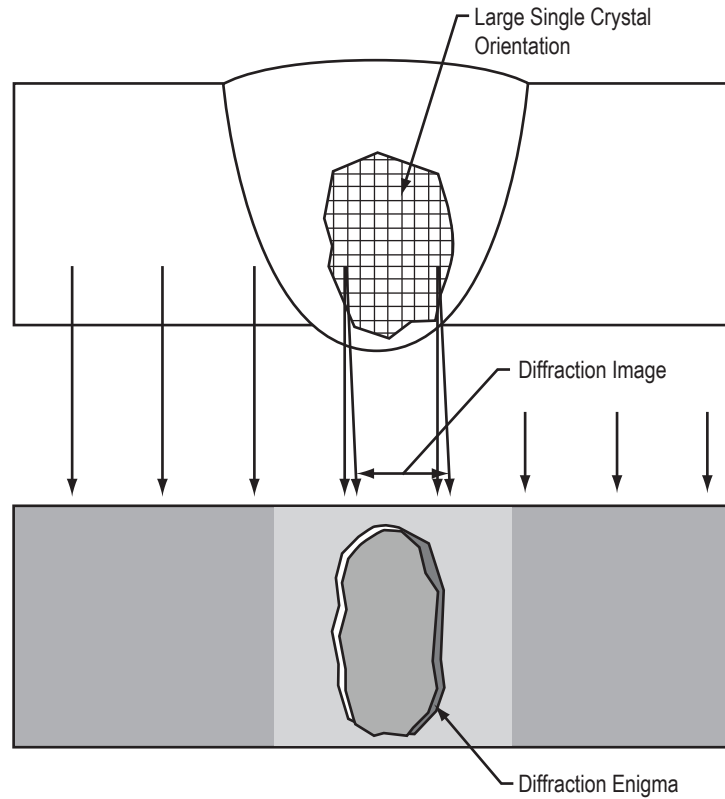


Figure 4. Diffraction effects from large grains can shift a noticeable portion of the power of a radiographic beam by a small angle. At one edge of the diffracted image of the grain, the shifted power adds to the background radiation, producing a dark image. At the other edge, the diffracted image subtracts, producing a light line. These boundaries are diffraction ‘enigmas,’ sharply enough defined to be visible when the edge of a large grain lines up parallel to the beam direction.

## 5. THE PLASMA TORCH THAT WOULD NOT SHIELD

### 5.1 Porosity in Aluminum Alloy Welds

Hydrogen can easily dissolve in the molten aluminum alloy of a weld pool after being liberated from small amounts of moisture or grease decomposed by an electric arc. The molten metal can dissolve more hydrogen than can the solidified metal. The excess hydrogen dissolved in the liquid tends to precipitate out as porosity upon solidification of aluminum alloy welds. The GTA process used to fabricate space vehicle tanks— despite stringent cleaning procedures, solvent wipedown, scraping, and white gloves—generates enough porosity that must be ground out and rewelded to be of economic concern.

### 5.2 Variable Polarity Plasma Arc Welding

Plasma arc welding can improve the situation. In this process, a ‘plasma gas’ is heated by an internal arc and then emerges through a water-cooled nozzle as a plasma jet, like the output of a little rocket engine. The stagnation pressure of the plasma jet is high enough so that it can penetrate to the bottom of the molten weld metal and melt more metal until it emerges out of the root of the weld in a little tongue of flame in what is called the ‘keyhole’ mode of welding. In the keyhole mode of welding, porosity-causing gaseous impurities tended to be entrained in the plasma. The welders claimed it was hard to make porosity in the keyhole mode.

However, the powerful affinity for oxygen of aluminum alloys presents a problem for plasma arc welding. The metal flowing back behind the plasma jet in its keyhole can easily be covered in a thin oxide layer with a quality like plastic film wrap, producing a trail of barely attached metal lumps in place of the desired weld. The remedy is to clean the surface of oxide using ‘reverse polarity,’ which is electrode positive and workpiece negative. A high-speed movie of the workpiece surface during reverse polarity operation GTA welding exhibits a field of sparkling mini-explosions. Apparently the mechanism by which cleaning takes place is by the explosive dielectric breakdown of oxide charged by the positive ions flowing from the plasma onto the oxide surface with an induced negative countercharge on the metal side, and not by sputtering, as has sometimes been asserted.<sup>11</sup>

A problem still exists with reverse polarity. The current is carried by slower moving heavy positive ions, which transfer less heat to the workpiece, while the lighter, faster electrons transfer a larger amount of heat to the electrode of the plasma torch. This reduces the usable welding power. Apparently, circuitry to vary the polarity was originally introduced by B.P. VanCleave, Boeing Co., starting in the late 1960s, creating the variable polarity plasma arc (VPPA) process, with its characteristic buzzing noise as the polarity is reversed. Investigations began at Marshall Space Flight Center (MSFC) with a commercial Hobart VPPA welding machine in 1979.<sup>12</sup>

### 5.3 The Strength of Variable Polarity Plasma Arc Welds

Welds made by the new VPPA process had a slightly lower tensile strength than GTA welds, although nowhere near enough to overcome its advantage over the GTA process. This was thought to be due to a more perpendicular orientation of the VPPA weld boundary to the tensile testing force axis, but there was a competing theory of ‘multiple pass strengthening’ that seized on a second difference between VPPA and GTA welds; VPPA welds were made with substantially fewer passes than GTA welds. As the strengths of both VPPA and GTA welds were very well documented empirically, it was not considered necessary to incur the expense of pursuing the cause of this difference.

Any attempt to understand the strength of welds must, of course, treat welds holistically. It will not do to merely consider the parts. The reader will recall that the strength of a brazed joint is in no way dictated by the strength of the braze metal. Brazed joints are generally much stronger than braze metal, a feature of the joint structure. The Soviets were long active in weld studies, and a simple ‘soft-interlayer’ model<sup>13</sup> applicable to aluminum alloy welds was developed by O.A. Bakshi et al. at Chelyabinsk Polytechnic Institute in the early 1960s.

### 5.4 Shield Gas Turbulence

It is consonant with our portrayal of welding as a highly multidisciplinary endeavor to conclude the treatment of VPPA welding by using this approach to solve a mystery. Welding engineers at MSFC redesigned the VPPA welding torch so as to eliminate water coolant joints and, in so doing, to eliminate chances for leakage problems. The redesigned torch worked very well up to a point, but the inert gas shielding failed (and the weld metal began to oxidize) at higher shield gas flow rates. Technicians adjusted the torch but could not make it work. What could be wrong? Of course, it was obvious to someone with a background in fluid mechanics. The designers had changed the exterior shape of the plasma nozzle (from which the shield gas flows in the interior of the shield gas cup) from conical to spherical. As shown in figure 5, the new exterior of the plasma nozzle allowed the shield gas separation point and the associated turbulent wake to move far enough out into the shield gas at high shield gas flow rates to reach the gas/atmosphere interface, where the turbulence began to entrain air and mix it into the shield gas. After observation of torch gas flow by spark photography to confirm the hypothesis, the nozzle exterior was put back the way it was and the problem disappeared.

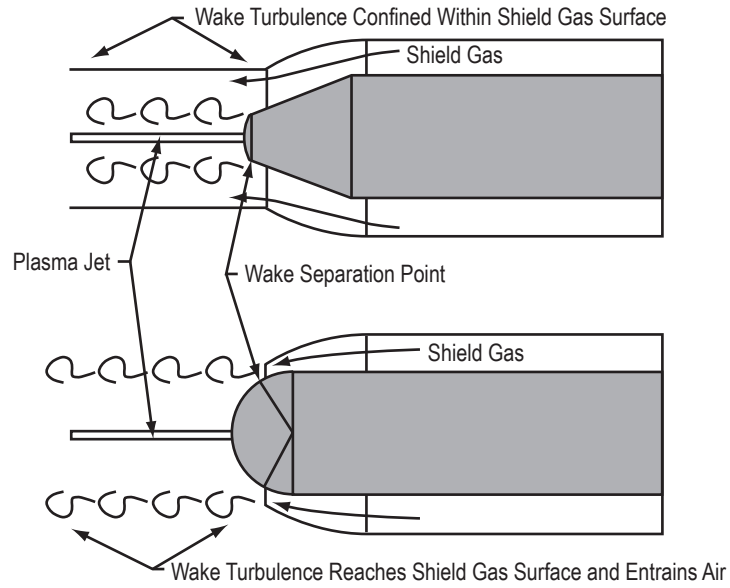


Figure 5. The external shape of a plasma jet nozzle makes a difference in torch performance. A spherical shape allows the wake separation point to move close enough to the shield gas surface at high flow rates for the wake turbulence to entrain atmospheric contamination (and lose shielding). A conical shape confines the turbulent wake deep within the shield gas flow, avoiding atmospheric entrainment even at high shield gas flows.

## 6. SPARKING AND SPATTER IN SPACE

Welded joints are inherently lightweight and gas tight. A safe and easy-to-use welding process could be very handy for making repairs in space or fabricating large structures from parts small enough to be carried up in practical-sized space vehicles.

### 6.1 The Soviet Universal Hand Tool

Although some electron beam welding experiments were carried out on Skylab (launched in 1973), the development of space welding was pioneered by the Paton Electric Welding Institute at Kiev, initially under the Soviets and later the Ukrainians. In October 1969, the Soviets made the first space welds with their ‘Vulkan’ automatic welding unit in a depressurized bay on the spacecraft Soyuz-6. It could operate in three modes—electron beam, low-pressure confined plasma, and consumable electrode. In July 1984, Svetlana Savitskaya and Vladimir Dzhanibekov carried out extravehicular trials of a hand-held electron beam Уинверсальный Ручной Инструмент on space station Salyut-7. NASA now refers to this instrument as the Universal Hand Tool (UHT).

The UHT emits an 8-kV beam that is defocused to avoid the deep penetration of a vapor cavity, which would make the welding process too sensitive to control by hand. The process takes advantage of the vacuum of space, necessary for the passage of an electron beam. The UHT is designed to cut and spray metal as well as to weld, this versatility being the occasion of the name ‘universal.’ A current advanced version, the product of a series of improving modifications, is available from the Paton Electric Welding Institute.

A workshop on space welding was held in 1989.<sup>14</sup> The International Space Welding Experiment (ISWE) was planned as a joint venture between NASA and the Paton Welding Institute, in which the UHT was scheduled to be tested aboard the space shuttle in 1997. Due to a scheduling problem caused by time lost when a hatch failed to open on a previous flight, ISWE was never flown, but a large part of the 1990s was spent preparing for it. The emphasis was on safety issues, and the welding group had to defend the safety of ISWE before a Safety Board.

“Would the 8-kilovolt beam puncture a space suit?” asked the Board. Swatches of a ceramic cloth intended as part of a protective garment for space welding were exposed to the 8-kV beam at various distances.<sup>15</sup> The expectation was that the electrons would rapidly coat the insulating fabric until the voltage would be sufficient to repel further incursions of electrons and that nothing further would happen. Instead, the beam sometimes did shoot holes in the fabric, with an accompanying flash, but only sometimes and after a substantial delay. Delay time depended upon standoff distance from the fabric. Minimum delay time of 6 to 8 s resulted from standoff distances of 0.5 to 2 ft. Longer and shorter standoff distances both yielded longer and longer delays. At 2 in, delays around 30 s were observed; at 4 ft, no burn-throughs were observed.

## 6.2 Arcs and Paschen Curves

After some thought and computation, the interpretation was that a fraction of the beam power was transmitted to the negative-charged fabric by positive ions generated by collisions between electrons in the beam and gas contaminant atoms in the less-than-perfect vacuum in which the experiment was performed. The flash was an indication of arcing in an atmosphere emitted from the fabric heated by the positive ion beam. In space, arcing is a very real hazard, not just in welding, but anywhere electric power is transmitted or where static electricity may accumulate.

An arc comprises an avalanche of electrons. When electrons are accelerated by an electric field to energies high enough to knock still more electrons out of ambient gas atoms, an avalanche of electrons is produced. An arc can absorb a great deal of energy from an electric field and impart it to an anode. Arcing will not occur if the gas is so dense that, between collisions, the electric field is inadequate to impart enough energy to an electron to knock further electrons out of an ambient gas atom. Arcing will not occur if the gas is so rarified that an electron emitted at a cathode (perhaps knocked out by a passing photon) reaches an anode before colliding with any ambient gas atom. Arcing will not occur, regardless of pressure, if the voltage is insufficient to impart enough energy to produce ionization over the entire gap between cathode and anode. Given a voltage difference ( $V$ ) between two metal surfaces separated by distance ( $d$ ), the electric field in the gap is

$$\frac{V}{d} . \quad (11)$$

At a given electric field, arcing can occur over a range of pressures bounded by a curve:

$$\frac{V}{d} = f(P) \quad (12)$$

or, more commonly,

$$V = f(Pd) . \quad (13)$$

Equation (13) is called a Paschen curve, named after the German physicist L.K.H.F. Paschen (1865–1947). See figure 6. It applies for a specific gas and a flat Cu electrode configuration.

Under normal atmospheric conditions, points ( $V$ ,  $P$ ,  $d$ ) are far to the right. To ‘strike an arc’ in the most commonly used welding process, shielded metal arc welding (SMAW), where the electrode is consumed to become part of the weld and the coating of the electrode decomposes to shield the hot weld metal from the atmosphere, the electrode is touched to the surface of the work-piece and  $d$  is reduced enough to induce arcing conditions. If a vacuum is pulled on an operating plasma torch, the arc jet retreats inside the torch and incinerates the torch. Under the high vacuum conditions of space, points ( $V$ ,  $P$ ,  $d$ ) are to the left. A bit of gas leakage can induce arcing. Longer arc paths may be favored over shorter ones.

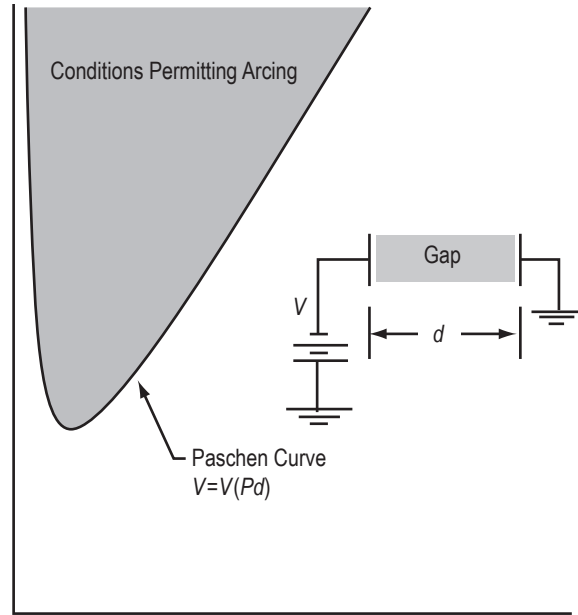


Figure 6. The Paschen curve  $V = V(Pd)$  bounds the values of voltage ( $V$ ), pressure ( $P$ ), and gap width ( $d$ ) for which arcing occurs in a specific gas. To the right, electron collisions occur so frequently with the gas that they do not build up enough kinetic energy to knock out other electrons. To the left, there are too few gas atoms in the gap for significant multiplication of electrons.

First efforts at producing a ‘hollow cathode’ low-voltage alternative to a high-voltage electron beam welder turned out to be rather prone to arcing. A hollow cathode welder uses a trickle of low-pressure inert gas over the cathode to enable a powerful low-voltage discharge. Whoever recalls vacuum tube electronic technology will recall that to get a substantial current discharge in a vacuum tube requires a high voltage due to an inhibiting space-charge buildup at the cathode surface. On the other hand, gas-filled power tubes can pass large currents at low voltage by neutralizing the space charge. Hollow cathode arcing presumably occurred at local pressure concentrations due to minute gas leaks. When due care is taken to control leaks, hollow cathode welders are quite feasible.

So how dangerous is the electron beam itself? First, it is difficult to see how the beam could be held steady for a dwell time sufficient to provoke arcing by accident, even under the low vacuum chamber conditions. Merely sweeping the beam across fabric would hardly be sufficient. Second, the vacuum in the test chamber being appreciably lower than that anticipated in space, the arcing tendency in space should be much less.

### 6.3 Weld Spatter

“Could weld spatter damage a spacesuit?” the Board wanted to know. Teflon-coated spacesuit outer covering fabric exposed to liquid metal droplets of various size were seen to produce a vapor that repelled the liquid metal. Unless the metal was trapped against the fabric, gradual deterioration would be anticipated rather than catastrophic damage. Nevertheless, could weld spatter be eliminated?

Weld spatter comprises tiny pieces of molten metal hurled away from the molten weld puddle when gas bubbles emerge at the metal surface. When a bubble breaks the surface, the surface tension of the depression left in the molten metal surface acts like the stretched bands of a slingshot, accelerating surrounding molten metal and causing it to rise above the molten surface. Spatter is the expelled metal droplets that detach and shoot away from the surface. It is limited by the size of the bubbles. Because vigorous evaporation cooling sets in at superheats substantially above melting, temperatures for the weld pool and the point at which spatter droplets are emitted are close to the melting temperature of the weld metal.

If, by careful control of cleanliness and diligent prior outgassing of weld materials, gas porosity with its attendant spatter is eliminated, a second possible source of weld spatter exists—a sudden exposure of already hot metal to the full force of a high-energy density heat source like an electron beam. This is reminiscent of the sudden, violent evaporation of superheated liquid, which sometimes occurs in liquids heated in a microwave oven, and, as in the case of coffee in a microwave oven, it is avoided by careful user technique. The author recalls how a sudden retraction of focal point of an electron beam left a crater in the crown of a weld bead. But the electron beam of the UHT is defocused. It is anticipated that education in the avoidance of this kind of spatter would normally be included in preflight astronaut training.

All these potential hazards derive from arcs and molten metals. Recently, a type of solid-state welding has become popular that eliminates arcs and molten metals—the friction stir weld (FSW) process. Currently, large forces are needed to wield this tool, but research is under way to determine whether this process can be adapted for space welding.

## 7. WELDING WITHOUT MELTING

Unanticipated welding problems emerged when new lighter, stiffer, stronger alloys (made by adding lithium (Li) to aluminum) came into use for space vehicle tanks. Speaking very broadly, ‘more highly alloyed’ metals tend to be harder due to more obstacles to dislocation motion, but have a tendency to grain boundary melting at temperatures close to melting due to segregation of alloying elements to grain boundaries. This can mean a tendency to grain boundary liquation cracking at high temperature, which can cause welding problems. In addition, Li compounds are known for capability to store and release hydrogen, and the alloy exhibited a tendency to secondary porosity; i.e., porosity absent in newly solidified metal, but emergent upon reheating.

### 7.1 The British Friction Stir Welding Process

In 1994, an investigation was initiated to explore the possibility of circumventing fusion welding problems by switching to a FSW solid state welding process patented in 1991<sup>16</sup> by The Welding Institute in Cambridge, England. In the FSW process, a rotating pin, usually threaded, is translated along the weld seam and stirs the seam together as it goes. See figure 7. So that the pin welds (and does not merely plow up the weld metal), a shoulder attached to the pin presses down on the weld metal adjacent to the pin. The weld metal is supported during welding by a platform, the ‘anvil,’ which has to be heavy due to the high ‘plunge’ force (typically a few tons) pushing the pin and shoulder down onto the workpiece.

In 1999, MTS Systems Corporation devised the self-reacting FSW tool now in common use.<sup>17</sup> The self-reacting FSW tool has two shoulders that sandwich the weld, one bearing on the weld crown and the other on the weld root. The shoulder at the weld root is fastened to the FSW pin, which passes through the workpiece and through the crown shoulder, which can be moved along the pin to squeeze the workpiece in a pinch force that takes the place of the plunge force in conventional FSW. The crown and root forces essentially balance one another, leaving little net plunge force to be absorbed by a fixture.

Initially, the weld metal flow was something of a mystery, and one still hears the term ‘chaotic flow’ for some FSW structures. Now, a clear understanding of basic flow patterns and the weld structures generated has been attained and work is under way to determine the mechanisms of formation of subtler structural features, particularly weld defects.

The breakthrough in understanding FSW flow was the realization that the main deformation was taking place over a very narrow ‘adiabatic’ shear band, the ‘shear surface,’ enclosing the tool and separating a plug of metal sticking to the tool from the stationary weld metal surrounding it. (Similar shear surfaces are observed in metal cutting.) An abrupt change takes place across the shear surface, going from relatively coarse parent metal grains to very fine grains. Flow streamlines pass through the shear surface, arc around the tool in the rotating plug, pass out through the shear surface, and are abandoned to the wake of the tool.

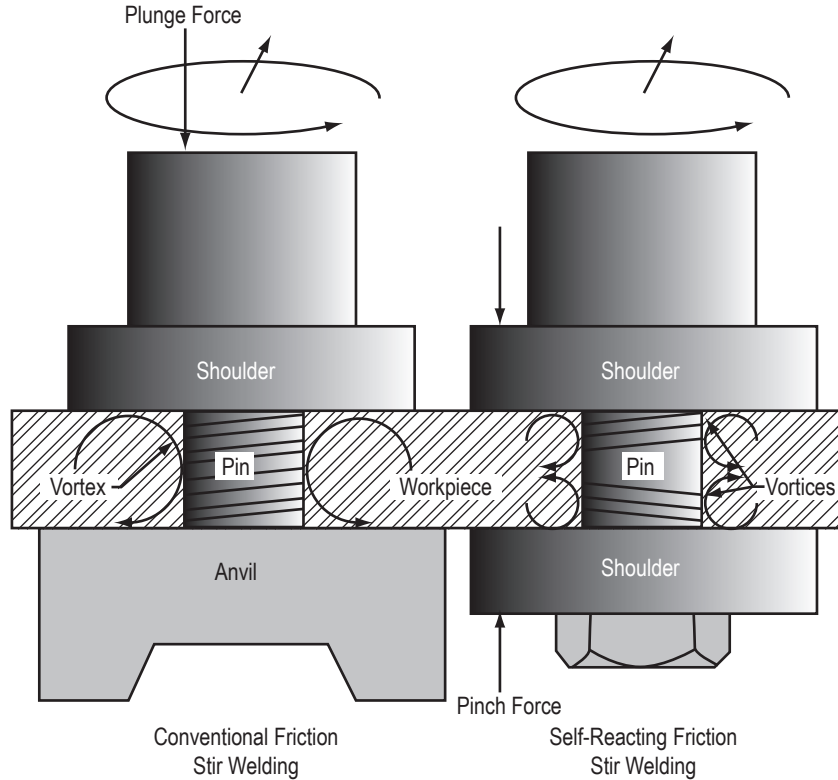


Figure 7. In friction stir welding, a rotating pin stirs the sides of a weld seam together. A shoulder prevents the upwelling of metal around the pin, which would result in plowing, not welding. In conventional FSW, a large plunge force maintains proper shoulder contact; it is balanced by a heavy fixed anvil underneath the workpiece. In self-reacting FSW, a pinch force maintains proper shoulder contact, making a heavy supporting anvil unnecessary.

## 7.2 How Does Friction Stir Welding Work?

How does the tool weld? Solid state welding processes work by bringing metal surfaces into contact at the atomic level. These surfaces must be clean and unobstructed, and they must be subjected to pressure adequate to compress any surface asperities and bring the surfaces into full contact. As a length of weld seam  $V\Delta t$ , where  $V$  is the weld speed and  $\Delta t$  is a time increment, crosses the shear surface, it is accelerated to the rotational speed  $R\Omega$  of the rotating plug of metal attached to the tool, where  $R$  is the radius of the shear surface and  $\Omega$  is the angular velocity of the tool. See figure 8. If the acceleration is uniform, the seam increment  $V\Delta t$  is stretched out to approximately

$$\frac{1}{2}R\Omega\Delta t \quad (14)$$

at the shear surface, increasing the area by a factor of approximately

$$\frac{1}{2} \frac{R\Omega}{V} \quad (15)$$

A typical order of magnitude of

$$\frac{R\Omega}{V} \sim 50 \quad (16)$$

amounts to a surface that is at least 96% bondable (24 clean areas to 1 contaminated area). Given a pressure on the surface approximately three times the tensile flow stress of the metal at the shear surface temperature or greater to ensure good surface contact, one may expect a sound weld from the friction stir process.

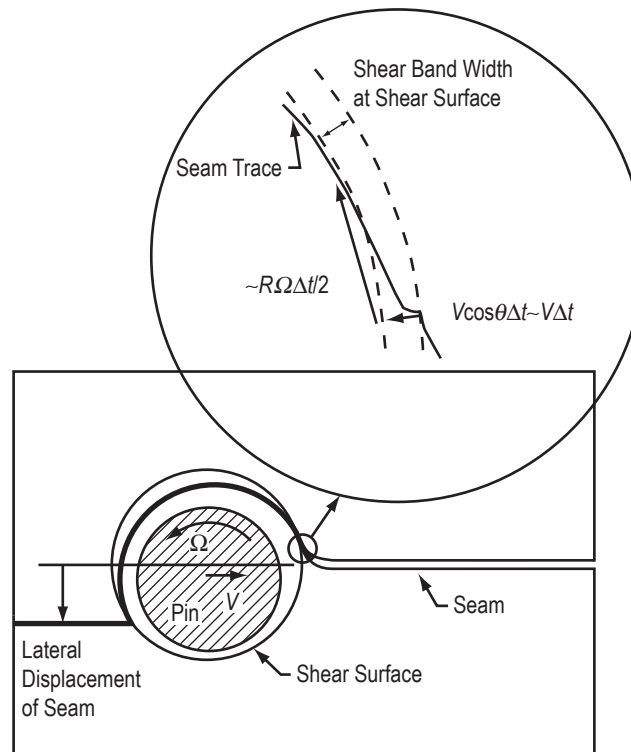


Figure 8. Plan view of trace of seam around pin during FSW in simplified two-dimensional flow model. An eccentricity  $\delta$  of the shear surface accommodates the backflow of metal around the pin. Metal inflow volume en route at weld speed  $V$  for a shear surface of unit height and radius  $R$  is  $2RV$ . Backflow at the outer edge of a plug of metal rotating with the tool at angular velocity is  $\delta R\Omega$ .

### 7.3 A Kinematic Model of Friction Stir Welding Metal Flow

If the volume rate at which metal encounters the tool, approximately  $2RV$ , is equated to the volume rate of backflow, approximately  $\delta R\Omega$ , around the tool, the eccentricity  $\delta$  of the shear surface can be estimated:

$$\delta \sim \frac{2V}{\Omega} . \quad (17)$$

The lateral displacement of the seam trace shown in figure 8 may be attributed to a ring vortex flow encircling the tool. The rotations in radial sections of the vortex ring are shown in figure 7. The ring vortex flow is driven by pin threads, shoulder scrolls, and, it appears pending further study, by any axial flow component up or down a smooth pin with axis tilted away from the vertical.

The lateral displacement of the seam trace can be estimated from a kinematic model combining displacements of an element of seam within the rotating plug. There is a displacement due to tool velocity ( $V$ ), tool rotation ( $\omega$ ), and ring vortex circulation, represented in plane section by a radial velocity component ( $v$ ). With radius  $r$  and angle  $\theta$  from tool motion direction representing the position of an element of weld seam in polar coordinates, the radial and circumferential velocities inside the rotating plug can be computed:

$$\frac{dr}{dt} \approx -V \cos\theta + v \quad (18)$$

$$\frac{rd\theta}{dt} \approx r\omega + V \sin\theta . \quad (19)$$

Equation of the time increment in equations (18) and (19) yields the differential equation for the streamline of the seam trace within the rotating plug. A further approximation can be made if, as in equation (16), the translational weld speed is much smaller than the surface rotation speed of the tool:

$$dr \approx \left( \frac{-\cos\theta + \frac{v}{V}}{1 + \frac{V}{r\omega} \sin\theta} \right) \frac{V}{\omega} d\theta \sim \left( -d \sin\theta + \frac{v}{V} d\theta \right) \frac{V}{\omega} . \quad (20)$$

The seam enters the rotating plug at radius  $R$  and angle  $\theta_o$ , is initially buried beneath successive deposits of weld metal on the plug ( $dr$  negative), is eventually uncovered ( $dr$  positive), and is finally abandoned when the radius is again  $R$  ( $dr=0$ ) and the angle is  $\theta$ , which can be found from equation (20). The maximum change in  $r$  is small compared to  $R$  (see eqn. (17)), and converting from polar coordinates, the lateral displacement  $y - y_o$ , positive toward the retreating side of the tool, can be estimated:

$$y - y_o \approx R \frac{v}{V} (\theta - \theta_o) . \quad (21)$$

In typical welds radial velocity  $v$  is negative (inward) near the shoulder and positive (outward) at the pin end (conventional) or center (self-reacting). The seam trace then is displaced to

the advancing side of the tool near the shoulder and to the retreating side at the bottom of the pin (conventional) or the pin center (self-reacting).

Note that if the shear surface radius  $R$  or the weld speed  $V$  varies in equation (20), the displacement will also vary. These variations will be periodic and may produce lateral waves as well as interruptions in weld streamlines. Variations in  $R$  could be produced by changes in shoulder contact from sticking to slipping; this would produce a lateral dispersion of tracers mainly close to the shoulder.

All this is seen in the steel shot tracer patterns produced at Boeing Co. and published in 1999 by K. Colligan.<sup>18</sup> Periodic emissions of weld metal from under the shoulder produce the ‘tool marks’ in the wake of the weld, as well as internal banding seen as the oval ‘onion ring’ pattern on a transverse section of the weld. Variations on the theme are presented by other tracers, such as a lead wire that melts and disperses in ‘wisps’ along the ‘tool marks’<sup>19</sup> and a tungsten wire that breaks into segments.

#### 7.4 Particle Interactions

In order to push an indenter into a metal surface, a pressure on the order of three times the flow stress of a tensile specimen is needed, due to the constraint of the metal surrounding the indentation. (This is an approximate result obtained from plastic slip-line theory.<sup>20</sup>) The same pressure is needed to push a surface asperity in and hence is needed on the seam trace at the tool if the seam is to close and form a sound weld. Plastic flow past an inclusion may be anticipated to exert about double the pressure, six times the tensile flow stress, on the inclusion, if the flow is visualized as a positive indentation forward and a negative indentation behind, each requiring three times the tensile flow stress. Particles passing through the shear interface may be treated as beams loaded by opposing pressures to determine whether or not they will be fractured by the flow. It is not a matter of ‘random’ chewing up of particles. What happens to embedded particles is the result of an orderly process subject to analysis, as is tool wear caused by these particles. Particle trajectories as estimated above and metal supporting forces determine whether they will gouge out abrasive wear trenches and how deep, etc.

#### 7.5 Torque and Drag Forces

If the shear surface shape is given in cylindrical coordinates, radius ( $r$ ), and depth ( $z$ ), by relation  $r(z)$ , and if the shear stress at the shear surface is roughly constant, then the torque ( $M$ ) required to operate the tool is

$$M \approx \int_{\text{Shear Surface}} 2\pi\tau r^2 \sqrt{dr^2 + dz^2} . \quad (22)$$

The mechanical power input to the weld is essentially  $M\Omega$ , where  $\Omega$  is the tool angular velocity; the power input to move the tool against the drag force is not generally significant in comparison. The power requirement for making an FSW is not very different from that needed

to make the equivalent fusion weld. Why should this be? The power input for both fusion and friction stir welds is principally determined by the requirement that it make up for heat losses to workpiece, tool, and fixture, which losses generally overshadow the contribution to weld metal structural changes. Given the same penetration depth, the surface of the molten metal pool of a fusion weld is very roughly the same as the shear surface of a friction stir weld. The temperature of these surfaces is very roughly the same, say  $T_m$ , the melting temperature of the weld metal, for the fusion weld and perhaps  $0.8 T_m$  for the shear surface. Hence the heat loss to the workpiece and fixture, the major heat loss, from similar embedded surfaces at similar temperatures ought to be very roughly the same.

Further, the power remains roughly constant even when the rpm is changed, so that the power is inversely proportional to the rpm. This is because the shape and temperature of the shear surface changes little with rpm and hence the heat losses, which have to be made up to maintain welding conditions, remain about the same. Of course, if power is constant, the torque must drop as the rpm rises. The rise in rpm must be accompanied by the small temperature rise needed to reduce the temperature sensitive shear stress and the torque to appropriate levels. So the power is not quite constant, but increases somewhat with rpm. But the power increase is small compared to the overall power because of the sensitivity of the shear stress to small changes in temperature.

The drag force ( $F_d$ ) on the tool may be estimated from an integral of pressure and shear forces over the surface of the shear surface:

$$F_d \approx \iint Pr \cos\theta d\theta dz - \iint \tau r \sin\theta d\theta \sqrt{dr^2 + dz^2} \quad . \quad (23)$$

Note that the weld metal is swept back with the tool rotation where the metal is hot and the flow stress is low and does not flow back according to the indentation model. The drag force behaves in a complicated way; sometimes it declines with rpm, sometimes it rises. The drag equation (23) yields no drag at all unless pressure ( $P$ ) and/or flow stress ( $\tau$ ) varies with  $\theta$  along the circumference of the shear surface. Tentatively, it appears as if there may be a pressure drag that is reduced by rpm and a shear drag that rises with rpm, but not enough data has been analyzed yet to be confident.

## 7.6 Weld Defects

Insufficient space is available to present more physics as they pertain to FSW, but it should be clear that the basics of the process are pretty well understood. Currently, the main research effort is devoted to understanding specific weld defects and problems.

For example, hollow tube-like defects called ‘wormholes’ are sometimes encountered inside welds. The ring vortex flow component brings tracer surface metal from the metal surface into the interior of the weld and is currently a suspect in the formation of wormholes. Could it be that wormholes are formed when seam gaps at the crown of the weld pass under the tool shoulder too far out to be subjected to adequate pressure to bring their surfaces into full contact? Might such gaps become entrained with the ring vortex flow into the weld interior, where they may become wormholes?



## 8. CONCLUSION

A few welding problems and processes have been presented here, including penetration, microfissures, enigmas, shielding mechanics, space welding, and FSW. Each situation has been understood and made tractable by applying an appropriate physical discipline.

Other approaches to tractability could have been taken. Cut-and-try plus statistical analysis is popular, a potential universal approach, but it depends more than one might think upon physical understanding, without which it is often unsuccessful, particularly in complex situations. Consultation with external experts may be effective, but, depending upon the discipline of the expert picked, one is likely to receive rather different understandings of the problem. Extradisciplinary factors may be dismissed as unexplained fluctuations.

The importance of breadth in the welding engineering education needed to treat uncategorized welding problems and processes (as they are encountered in nature) is striking. The applications cited above call up heat transfer, thermal stresses, solidification theory, segregation theory, optics/diffraction, fluid mechanics, electromagnetic theory, and plasticity theory. This seems a tall order for a baccalaureate welding engineering curriculum, particularly when a bit of mathematics is generally needed to verify initial physical insights.

But if the welding engineer who takes the first cut at it should pigeonhole a problem in the wrong discipline, a great deal of money may be spent without ever obtaining a useful solution. Specialists cannot be relied upon at the outset; the initial task is to select the right specialist. Nor can all-purpose statistical methods be relied upon. Asking the right questions of statistics requires physical expertise and understanding. If any substitute exists, the author is unaware of it.

## REFERENCES

1. Newton, I.: *Philosophiae Naturalis Principia Mathematica*, London: Joseph Streater for the Royal Society, 1687.
2. Lagrange, J.-L.: *Méchanique analitique* (sic), Paris: Chez la Veuve Desaint, 1788.
3. Morrison, T.J.; Shira, C.S.; and Weissenberg, L.A.: “The Influence of Minor Elements on Alloy 718 Weld Microfissuring. Effects of Minor Elements on the Weldability of High-Nickel Alloys,” *Proceedings of a Welding Research Council Symposium*, Houston, TX, October 3, 1967.
4. Lucas, M.J., Jr.; and Jackson, C.E.: “The Welded Heat-Affected Zone in Nickel Base Alloy 718,” *Welding Journal*, Vol. 49, No. 2, p. 46-s, 1970.
5. Lambert, J.A.: “Cast-to-Cast Variability in Stainless Steel Mechanized GTA Welds,” *Welding Journal*, Vol. 70, No. 55, pp. 41–52, 1991.
6. Nunes, A.C., Jr.: “Weld Puddle Physics,” Unpublished Report: ASEE-NASA Summer Faculty Fellowship Program, 1975.
7. Nunes, A.C., Jr.: “An Extended Rosenthal Weld Model,” *Welding Journal*, Vol. 62, No. 6, pp. 165-s–170-s, 1983.
8. Heiple, C.R.; and Roper, J.R.: “Mechanism for Minor Element Effect on GTA Fusion Zone Geometry,” *Welding Journal*, Vol. 61, No. 4, pp. 97-s–102-s, 1982.
9. Marangoni, C.: “Ueber die Ausbreitung der Tropfen einer Flüssigkeit auf der Oberfläche einer anderen,” *Annalen der Physik und Chemie*. CXLIII(7), pp. 337–354, 1871.
10. Walley, J.L.; Nunes, A.C.; Clouch, J.L.; and Russell, C.K.: “Study of Radiographic Linear Indications and Subsequent Microstructural Features in Gas Tungsten Arc Welds of Inconel 718,” *NASA/TM—2007–215075*, Marshall Space Flight Center, AL, September 2007.
11. Pang, Q.; Pang, T.; McClure, J.C.; and Nunes, A.C.: “Workpiece Cleaning During Variable Polarity Plasma Arc Welding of Aluminum,” *Journal of Engineering for Industry*, Vol. 116, pp. 463–466, 1994.
12. Nunes, A.C., Jr.; Bayless, E.O., Jr.; Jones III, C.S.; et al.: “Variable Polarity Plasma Arc Welding on the Space Shuttle External Tank,” *Welding Journal*, Vol. 63, No. 9, pp. 27–35, 1984.

13. Bakshi, O.A.; and Shron, R.Z.: "The Static Tensile Strength of Welded Joints with a Soft Interlayer," *Welding Production*, Vol. 9, No. 5, pp. 915, 1962.
14. Kuvin, B.F.: "Welding in Space: Questions Remain," *Welding Design and Fabrication*, pp. 22–24, May 1990.
15. Nunes, A.C., Jr.; Russell, C.K.; Zimmerman, F.R.; and Fragomeni, J.M.: "Low-Pressure Gas Effects on the Potency of an Electron Beam Against Ceramic Cloth," *NASA/TM—1999–209762*, Marshall Space Flight Center, AL, November 1999.
16. Thomas, W.M.; et al.: "Friction Stir Butt Welding," International Patent Application No. PCT/GB92/02203 and GB Patent Application No. 9125978.8, December 1991.
17. Campbell, C.L.; Fullen, M.L.; Skinner, M.J.: "Welding Head," U.S. Patent No. 6,199,745, March 2001.
18. Colligan, K.: "Material Flow Behavior During Friction Stir Welding of Aluminum," *Welding Journal*, Vol. 78, No. 7, pp. 229-s–237-s, 1999.
19. Schneider, J.; Beshears, R.; and Nunes, A.C., Jr.: "Interfacial Sticking and Slipping in the Friction Stir Welding Process," *Materials Science & Engineering A*, Vol. 435–436, pp. 297–304, 2006.
20. Johnson, W.; and Mellor, P.B.: *Plasticity for Mechanical Engineers*, D. Van Nostrand Company Ltd., pp. 330–334, 1962.

REPORT DOCUMENTATION PAGE			Form Approved OMB No. 0704-0188		
<p>The public reporting burden for this collection of information is estimated to average 1 hour per response, including the time for reviewing instructions, searching existing data sources, gathering and maintaining the data needed, and completing and reviewing the collection of information. Send comments regarding this burden estimate or any other aspect of this collection of information, including suggestions for reducing this burden, to Department of Defense, Washington Headquarters Services, Directorate for Information Operation and Reports (0704-0188), 1215 Jefferson Davis Highway, Suite 1204, Arlington, VA 22202-4302. Respondents should be aware that notwithstanding any other provision of law, no person shall be subject to any penalty for failing to comply with a collection of information if it does not display a currently valid OMB control number.</p> <p><b>PLEASE DO NOT RETURN YOUR FORM TO THE ABOVE ADDRESS.</b></p>					
1. REPORT DATE (DD-MM-YYYY) 01-10-2010		2. REPORT TYPE Technical Memorandum		3. DATES COVERED (From - To)	
4. TITLE AND SUBTITLE  Welding As Science: Applying Basic Engineering Principles to the Discipline			5a. CONTRACT NUMBER		
			5b. GRANT NUMBER		
			5c. PROGRAM ELEMENT NUMBER		
6. AUTHOR(S)  A.C. Nunes, Jr.			5d. PROJECT NUMBER		
			5e. TASK NUMBER		
			5f. WORK UNIT NUMBER		
7. PERFORMING ORGANIZATION NAME(S) AND ADDRESS(ES) George C. Marshall Space Flight Center Marshall Space Flight Center, AL 35812			8. PERFORMING ORGANIZATION REPORT NUMBER  M-1298		
9. SPONSORING/MONITORING AGENCY NAME(S) AND ADDRESS(ES) National Aeronautics and Space Administration Washington, DC 20546-0001			10. SPONSORING/MONITOR'S ACRONYM(S) NASA		
			11. SPONSORING/MONITORING REPORT NUMBER NASA/TM-2010-216449		
12. DISTRIBUTION/AVAILABILITY STATEMENT Unclassified-Unlimited Subject Category 26 Availability: NASA CASI (443-757-5802)					
13. SUPPLEMENTARY NOTES  Prepared by the Materials and Processes Laboratory, Engineering Directorate					
14. ABSTRACT  This Technical Memorandum provides sample problems illustrating ways in which basic engineering science has been applied to the discipline of welding. Perhaps inferences may be drawn regarding optimal approaches to particular welding problems, as well as for the optimal education for welding engineers. Perhaps also some readers may be attracted to the science(s) of welding and may make worthwhile contributions to the discipline.					
15. SUBJECT TERMS welding, weld defects, friction stir welding, conceptual models, mathematical models, finite element models					
16. SECURITY CLASSIFICATION OF:			17. LIMITATION OF ABSTRACT  UU	18. NUMBER OF PAGES 40	19a. NAME OF RESPONSIBLE PERSON STI Help Desk at email: help@sti.nasa.gov
a. REPORT U	b. ABSTRACT U	c. THIS PAGE U			19b. TELEPHONE NUMBER (Include area code) STI Help Desk at: 443-757-5802



National Aeronautics and

Space Administration

IS20

**George C. Marshall Space Flight Center**

Marshall Space Flight Center, Alabama

35812